

*Full Length Research Paper*

# Simple model to study the effect of temperature on the greenhouse with shading nets

C. Chen<sup>1\*</sup>, T. Shen<sup>2</sup> and Y. Weng<sup>3</sup>

<sup>1</sup>Department of Bio-industrial Mechatronics Engineering, National ChungHsing University, 250 Kuokuang Road, Taichung, Taiwan.

<sup>2</sup>Department of Biomechatronics Engineering, National Chia-I University, 1 Hsieh-Fu Road, Chia-I, Taiwan.

<sup>3</sup>Department of Bio-industrial Mechatronics Engineering, National ChungHsing University, 250 Kuokuang Road, Taichung, Taiwan.

Accepted 16 February, 2011

**Due to high solar intensity, the internal temperature of greenhouses in subtropical regions is so high that it is difficult for crops to survive. There are two types of shading nets that are applied to reduce the solar intensity entering the greenhouse. The purpose of this research is to develop a simple greenhouse model to describe the effect of these shading nets on the inside temperatures of a greenhouse. The thermal condition was assumed as the steady state. The detailed microclimate data of an experimental greenhouse with internal and external shading nets were collected during various weather conditions. The model was validated using experimental data collected from various conditions. The prediction accuracy of the model for air temperature was about 1.5°C. It is concluded that this model could be applied to evaluate the performance of shading nets and serve as a tool for the design of a subtropical greenhouse.**

**Key words:** Subtropical, greenhouse climate model, shading nets.

## INTRODUCTION

The application of greenhouse for crop production is very important in the world (Omer, 2009). In order to maintain an adequate microclimate for growth of crops and protection against rain and storms, the greenhouse has become popular in subtropical regions. However, high solar energy leads to heat accumulation in greenhouses especially in summer. The cooling strategy has become a useful technology for environmental control of a subtropical greenhouse.

There are four ways to solve the heat accumulation problem in greenhouses. These are: 1) ventilation, 2) shading, 3) evaporative cooling and 4) composite systems (Sethi and Sharma, 2007). With shading screens, the solar energy is retarded when entering the greenhouse. Thus, excessively high temperatures are reduced. Ventilation and evaporative cooling is also an effective way to remove the hot air from greenhouses (Chen,

2003; Oz et al., 2009). Negative pressure fans are the typical equipment to remove greenhouse heat. However, the walls of a greenhouse need to be kept closed at all times in order to apply these devices. The structure of a greenhouse should be strong enough to resist the side pressure that is induced by the mechanical fans. This may cause the construction cost of a greenhouse to increase.

Recently, a simple and inexpensive greenhouse has been introduced (Critten and Bailey, 2002; Impron et al., 2007), where by, the sidewall of the greenhouse is composed of insect screens and the roof is covered with transparent materials. This kind of greenhouse is referred to as a high tunnel in some literatures (USAID, 2008; van Heum and ven der Post, 2004). Two kinds of shading nets: internal shading and the external shading nets are utilized in these greenhouses. Internal shading nets are installed beneath the roof of the greenhouse and guard against bad weather conditions. External shading nets are installed at the position above the roofs. They can be used to reduce the total solar energy entering the greenhouse and to provide more space for plant growth

\*Corresponding author. E-mail: [ccchen@dragon.nchu.edu.tw](mailto:ccchen@dragon.nchu.edu.tw).  
Tel: 886-4-22857562. Fax: 886-4-22857135.

and development. However, these screens are susceptible to damage by the extreme weather conditions.

The structural analysis and the study of the functional characteristics of the greenhouse are prerequisite for greenhouse application (Emekli et al., 2010). A greenhouse climate model is a very useful tool to describe the relationship between the microclimates and the influencing factors. Several types of greenhouse models were reviewed by Kano and Saddle (1985). Froehlich et al. (1979) classified the greenhouse model as steady state, steady-periodic and time-dependant. Boulard and Baille (1993) incorporated the performance of evaporative cooling equipment into these models. Jolliet (1994) proposed an integrated model to consider the transpiration function of crops. Recently, more greenhouse models were proposed and validated. Roy et al. (2002) assumed the greenhouse as a perfectly stirred tank and studied the convective function and ventilation in a greenhouse. Fatnassi et al. (2003) investigated the effect of insect-proof screens on the microclimate of greenhouses. The leaf boundary-layer model was proposed and incorporated into the microclimate model by Boulard et al. (2004). The interactions between the banana crop and the surrounding microclimate were studied by Demrati et al. (2007). A detailed thermal model was developed and validated to evaluate the arch shape greenhouse by Sengar and Kothari (2008).

However, despite the many greenhouse models developed and validated, in the opinion of the authors, a greenhouse model that considered the effect of positions of shading nets is not yet available. The application of internal and external shading nets was so popular to reduce the solar radiation into the greenhouse and high tunnel. A greenhouse model that incorporates the shading effect needs to be developed and validated. This model could serve as a tool to evaluate the performance of these nets.

The objective of this study was to develop a simple model to describe the effect of the shading nets on the microclimate of a greenhouse. The microclimate data of the experimental greenhouse were collected to validate the model.

### Model development

The development of a greenhouse model for the utilization of shading nets was to divide the greenhouse into two layers. The schematic diagram of the thermal fluxes in a typical greenhouse is presented in Figure 1. The assumptions of this model are as follows.

1. No temperature gradient existed in each layer.
2. The heat transfer coefficients of cover materials were constant.
3. The temperatures of the internal air, crops and cover materials were in a steady state.

4. Crops were planted in medium containers, the ground was covered with weeds-inhibiting nets and the soil thermal energy was not considered because crops covered most parts of the floor.

5. Only the transmittance of shading nets was considered.

6. The air exchange rate between the upper parts and lower parts of internal shading nets was assumed as constant.

### Thermal transfer model of the upper layer

The thermal systems of upper and lower layer are denoted as "1" and "2", respectively.

#### The input energy

$$Q_{S1} = (1 - \tau_1) \tau_0 I_s \quad (1)$$

where  $Q_{S1}$  is the solar energy in the upper layer in  $Wm^{-2}$ ;  $\tau_1$  is the transmittance of internal shading nets;  $\tau_0$  is the transmittance of external shading nets; and  $I_s$  is the entrance energy of shortwave radiation from the sun in  $Wm^{-2}$ .

#### The output energy

a.  $Q_{1a}$ : energy flow in/out to ambient atmosphere by heat transfer

$$Q_{1a} = A_1 U_{w1} (T_1 - T_a) \quad (2)$$

where  $Q_{1a}$  is the energy flow to ambient atmosphere by heat transfer in W;  $A_1$  is the surface area of upper layer including the roof and partial wall in  $m^2$ ,  $U_{w1}$  is the heat transfer coefficient of greenhouse cover materials in  $Wm^{-2}K^{-1}$ ;  $T_1$  is the upper layer temperature in  $^{\circ}C$ ; and  $T_a$  is the ambient temperature in  $^{\circ}C$ .

b.  $Q_{12}$ : energy exchange between upper and layer

$$Q_{12} = A_s U_{12} (T_1 - T_2) \quad (3)$$

where  $A_s$  is the area of internal shading nets in  $m^2$ ;  $U_{12}$  is the heat transfer coefficient of internal shading nets in  $Wm^{-2}K^{-1}$ ; and  $T_2$  is the lower layer temperature in  $^{\circ}C$ .

c.  $Q_{m1}$ : energy exchange by mechanical ventilation

$$Q_{m1} = M_1 \rho C_p (T_1 - T_a) \quad (4)$$

where  $M_1$  is ventilation rate of mechanical devices in upper part is  $m^3s^{-1}$ ;  $\rho$  is the air density in  $kgm^{-3}$ ; and  $C_p$  is the air specific heat in  $J kg^{-1}^{\circ}C^{-1}$

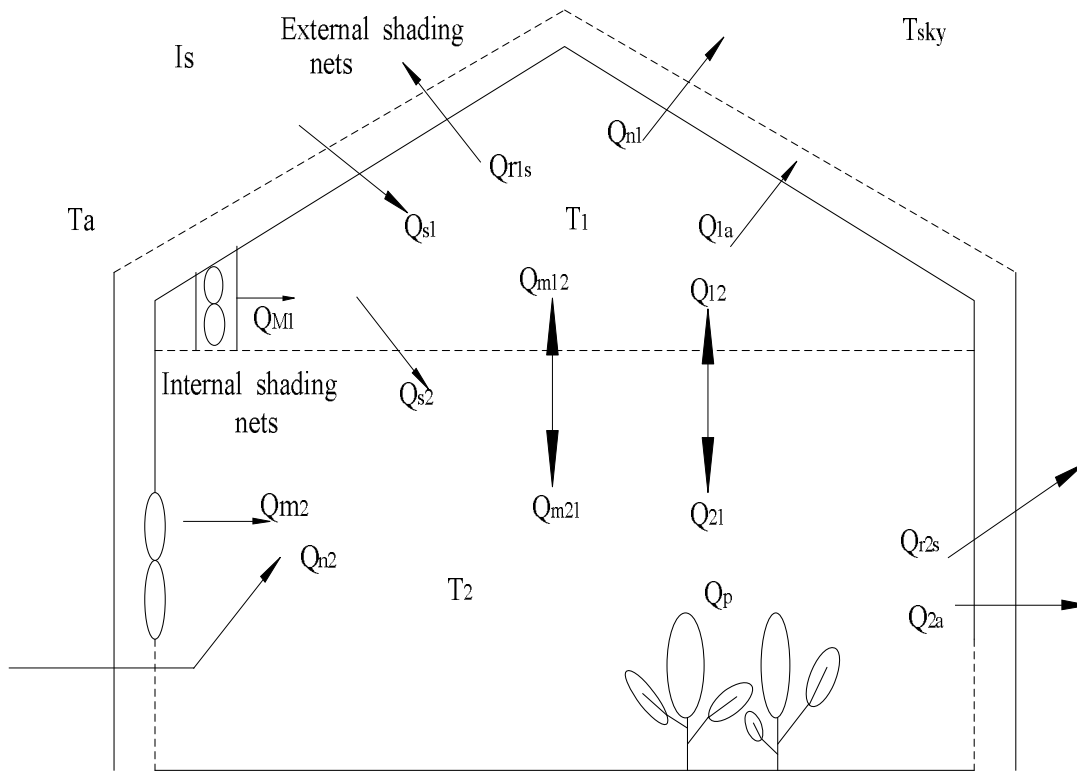


**Figure 1.** Schematic diagram of the thermal transfer model for a greenhouse with shading nets;  $I_s$ , entrance energy of shortwave radiation from the sun ;  $T_{sky}$ , sky temperature ;  $T_a$ , ambient temperature;  $T_1$ , upper layer temperature ;  $T_2$ , lower layer temperature ;  $Q_{s1}$ , the solar energy in the upper layer;  $Q_{1a}$ , energy flow in/out to ambient atmosphere by heat transfer;  $Q_{12}$ , energy exchange between upper and lower layer;  $Q_{m1}$ , energy exchange by mechanical ventilation;  $Q_{n1}$ , energy exchange by natural ventilation;  $Q_{m12}$ , energy exchange rate due to the air from the lower layer;  $Q_{r1s}$ , energy exchange by the radiation heat exchange;  $Q_{s2}$ , the solar energy in the lower layer;  $Q_{2a}$ , energy flow to ambient atmosphere by heat transfer;  $Q_{21}$ , energy exchange between lower and upper layer;  $Q_{m2}$ , energy exchange by mechanical fans;  $Q_{n2}$ , energy exchange due to natural ventilation;  $Q_{m21}$ , energy exchange from upper layer due to the mechanical ventilation of lower layer;  $Q_{r2s}$ , energy exchange by the radioactive heat exchange;  $Q_p$ , transpiration energy by crops.

d.  $Q_{n1}$ : energy exchange by natural ventilation

$$Q_{n1} = AR \rho C_p (T_1 - T_a) \quad (5)$$

where AR is the natural air exchange rate of greenhouse in  $m^3 s^{-1}$ . AR was calculated following the equation of Roy et al. (2002):

$$AR = 0.5A_{op} C_d (g (T_{ave} - T_a)H/2T_a)^{0.5} \quad (6)$$

$$T_{ave} = (T_1 V_1 + T_2 V_2) / (V_1 + V_2) \quad (7)$$

where  $A_{op}$  is the area of opening in  $m^2$ ;  $C_d$  is discharge coefficient;  $g$  is gravitational acceleration in  $ms^{-2}$ ;  $T_{ave}$  is the average temperature of greenhouse in  $^{\circ}C$ ;  $H$  is the opening height in  $m$ ;  $V_1$  is the volume of the upper layer in  $m^3$ ; and  $V_2$  is the volume of the lower layer in  $m^3$ .

e.  $Q_{m12}$ : energy exchange rate due to the air from the

lower layer

$$Q_{m12} = M_{12} \rho C_p (T_1 - T_2) \quad (8)$$

where  $M_{12}$  is the ventilation rate between the upper and lower layer due to the mechanical ventilation of upper layer in  $m^3 s^{-1}$ .

f.  $Q_{r1s}$ : heat transfer due to long-wave radiation

$$Q_{r1s} = \epsilon F_{1s} \sigma A_s (T_{1k}^4 - T_{sky}^4) \quad (9)$$

$$T_{sky} = 0.0552(T_{ak})^{1.5} \quad (10)$$

where  $\epsilon$  is the long wave thermal transmittance of cover materials;  $F_{1s}$  is the shape factors for the sky as seen from the upper layer;  $\sigma$  is the Stephan-Boltzman constant;  $T_{1k}$  is the absolute temperature of upper layer air in K;  $T_{sky}$  is the sky temperature in K; and  $T_{ak}$  is ambient air temperature in K. The energy balance

equation for the upper layer is:

$$Q_{S1} = Q_{10} + Q_{12} + Q_{m1} + Q_{n1} + Q_{m12} + Q_{r1s} \quad (11)$$

### The thermal transfer model of the lower layer

#### The input energy

A.  $Q_{S2}$ : input energy

$$Q_{S2} = T_1 T_0 I_s \quad (12)$$

#### The output energy

B. Output energy

a.  $Q_{2a}$ : energy flow to ambient atmosphere by heat transfer

$$Q_{2a} = A_2 U_{k2} (T_2 - T_a) \quad (13)$$

where  $A_2$  is the wall area of lower part in  $m^2$ ; and  $U_{k2}$  is the heat transfer coefficient of cover materials in  $Wm^{-2}K^{-1}$ .

b.  $Q_{21}$ : energy exchange between lower and upper layer

$$Q_{21} = A_s U_{12} (T_2 - T_1) \quad (14)$$

c.  $Q_{m2}$ : energy exchange by mechanical fans

$$Q_{m2} = M_2 \rho C_p (T_2 - T_a) \quad (15)$$

where  $M_2$  is the air exchange rate due to the mechanical fans in lower part in  $m^3 s^{-1}$ .

d.  $Q_{n2}$ : energy exchange due to natural ventilation

$$Q_{n2} = AR \rho C_p (T_2 - T_a) \quad (16)$$

where  $AR$  is the natural air exchange rate of greenhouse in  $m^3 s^{-1}$ .

e.  $Q_{m21}$ : energy exchange from upper layer due to the mechanical ventilation of lower layer

$$Q_{m21} = M_{21} \rho C_p (T_a - T_2) \quad (17)$$

where  $M_{21}$  is the ventilation rate between the upper and lower part due to the mechanical ventilation of lower layer in  $m^3 s^{-1}$ .

f.  $Q_{r2s}$ : heat transfer due to long-wave radiation

$$Q_{r2s} = \epsilon F_{2s} \sigma A_f (T_{2k}^4 - T_{sky}^4) \quad (18)$$

where  $F_{2s}$  is the shape factors for the sky as seen from

the lower layer;  $A_f$  is the floor area in  $m^2$ ; and  $T_{2k}$  is the absolute air temperature of lower part in K.

g.  $Q_{ab}$ : absorption of thermal energy of nets

$$Q_{ab} = \alpha (1 - \tau_1) T_0 I_s \quad (19)$$

where  $\alpha$  is the absorptance of internal nets

h.  $Q_p$ : crop transpiration

$$Q_p = \lambda Tr Pf Af \quad (20)$$

where  $\lambda$  is latent heat of vaporization in  $kJkg^{-1}$ ;  $Tr$  is transpiration rate of tomatoes in  $kgm^{-2}$ ; and  $Pf$  is the canopy area index. The transpiration model of tomatoes is adopted from the HORTITRANS model (Jolliet, 1994):

$$Tr = a I_s / \lambda + h_t (1 - RH) P_{ws} / (\lambda \gamma) \quad (21)$$

$$a = 0.154 \ln(1 + 1.1 LAI^{1.13}) \quad (22)$$

$$k_t = 1.65 LAI (1 - 0.56 \exp(-I_s/13.0)) \quad (23)$$

$$\gamma = 0.066 kPa K^{-1} \quad (24)$$

$P_{ws}$  was calculated following Weiss (1977):

$$P_{ws} = 0.61078 \exp(17.2694 * T_a) / (T_a + 237.3) \quad (25)$$

where  $RH$  is relative humidity in decimal; and  $LAI$  is leaf area index.

The energy balance equation for the lower layer is:

$$Q_{S2} = Q_{20} + Q_{21} + Q_{m2} + Q_{m21} + Q_{r2s} + Q_{ab} + Q_p \quad (26)$$

## EXPERIMENTAL DETAILS

### Greenhouses

A 12.8 × 32 × 3.5 m high, polycarbonate glazed steel framed structure greenhouse located at Wufeng, in Taichung was selected to validate the thermal transfer model. The transmittance was 50% for external and internal shading nets. The roof vents and side windows were operated with motors. The mechanical ventilation system consisted of 4 units of 40 cm fans with a capacity of 180  $m^3 min^{-1}$  at the upper layer and 4 units of 135 cm fans with a capacity of 550  $m^3 min^{-1}$  at the lower layer. The height of internal shading net was 3.0 m. The schematic of the experimental greenhouse is presented in Figure 2.

Tomatoes were planted in medium bags placed on the ground and crop spacing was 1.35 m. The ratio for the tomatoes to the floor was nearly 70%.

### Measuring devices

T-type thermocouples (Omega Engineering, USA) were applied to measure the upper, lower and ambient air temperature. The thermocouples junctions were placed in a radiation-shielded box

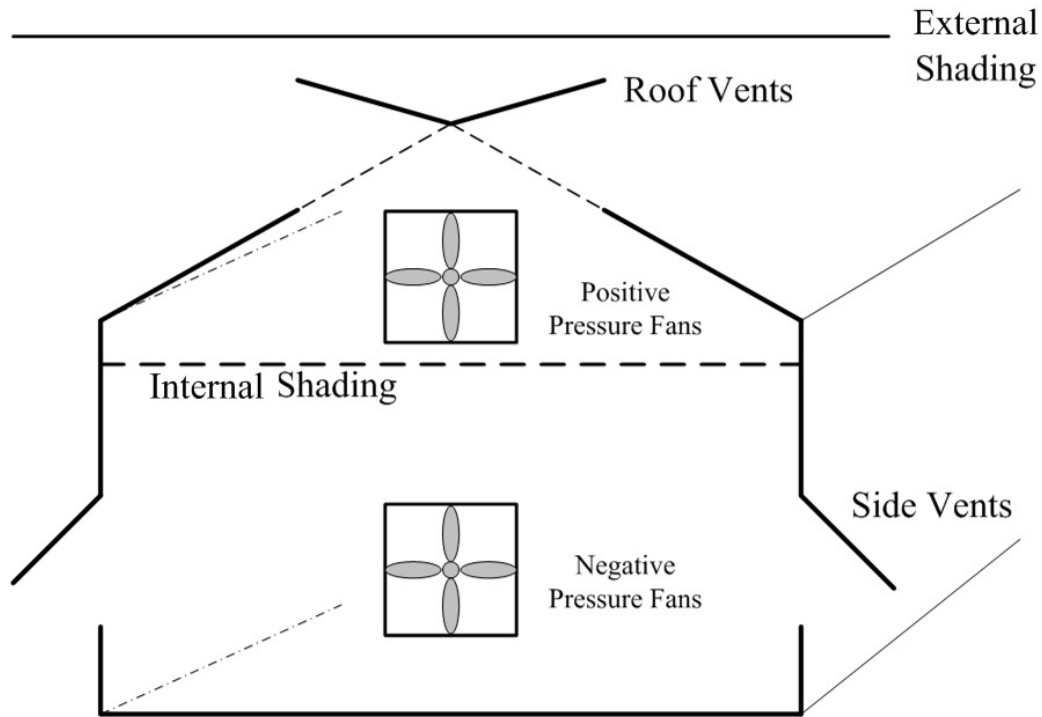


Figure 2. Schematic diagram of experiment greenhouse.

Table 1. Model input parameter for the greenhouse model.

Symbols	Description	Numeric values	Units
$U_{w1}$	Thermal transfer coefficient of roofs	6.1	$Wm^{-2}C^{-1}$
$U_{w2}$	Thermal transfer coefficient of walls	6.3	$Wm^{-2}C^{-1}$
$T_0$	Transmittance of the cover materials	0.8	
$T_i$	Transmittance of the inner shading nets	0.5	
$A_s$	Area of the internal shading nets	390	$m^2$
$U_{12}$	Heat transfer coefficient of the inner shading nets	0.2	$Wm^{-2}C^{-1}$
$C_d$	Discharge coefficient	0.35	
$M_{12}$	Ventilation rate of between upper and lower nets	0.1	$m^3s^{-1}$
$F_{1s}$	Shape factor for the sky as seen from the upper layer	0.85	
$F_{2s}$	Shape factor for the as seen from the lower layer	0.39	
$V_1$	Volume of the upper layer	512	$m^3$
$V_2$	Volume of the lower layer	1229	$m^3$
$\alpha$	absorptance of internal nets	0.04	

including an aspirated fan. All thermocouples were connected to a Delta-T 2e data logger (Delta-T Co., UK). The accuracy of these temperature sensors was maintained within  $0.15^\circ C$  after calibration with the temperature calibrator (TC-2000, Instrutek, AS Norway).

The air relative humidity was measured by the Shinyei THT-B121 resistive-type transmitter (Shinyei Kaisha Co., Tokyo, Japan). The accuracy of these sensors was kept within 0.7% after calibration with saturated salt solutions.

The solar radiation was detected by three E8-48 Pyranometers (Eppley Co., USA). The solar radiation at upper layer, lower layer and ambient atmosphere condition were recorded by the same data logger. The air velocity was measured by TSI 8450 air velocity transducer (TSI Co., St. Paul, MN USA). The measuring range was

from  $0$  to  $20\text{ ms}^{-1}$  and the accuracy was within 1.5% of reading. The leaf area index (LAI) was measured by LAI-200 Plant Canopy Analyzer (Li-COR, NL USA). The experimental design of this study included cases of no ventilation, natural ventilation and mechanical ventilation.

#### Parameters for the thermal transfer model

The physical parameters for this study are listed in Table 1. Most of the parameters were obtained from the manufacture's specification. Only the air ventilation rates were measured in the study. Five air velocity transducers were placed below the internal net. The

ventilation rate between the upper and lower layer was calculated by the average air velocity and the area of internal net.

### Simulation

In this study, two unknown temperatures,  $T_1$  and  $T_2$  were calculated from two equations, Equations 11 and 26. As the temperature involved the fourth power term  $T_{ik}^4$ , the  $T_1$  and  $T_2$  values could not be directly calculated by algebraic method. The calculation of AR values also involved the  $T_1$  and  $T_2$  value. A Q-BASIC program (NETS.BAS) was written by the authors to do the computing work. The iterative method was applied and two temperatures were determined using the following procedures:

1. Input the ambient conditions including air temperature, relative humidity and solar radiation.
2. Input the air exchange rate of mechanical ventilation if necessary.
3. Input two initial values ( $T_{10}$  and  $T_{20}$ ).
4. Calculate the natural air exchange rate by Equations 6 and 7.
5. Calculate the first iterative value of  $T_{11}$  by Equation 11.
6.  $T_{11}$  and  $T_{20}$  were the initial condition to calculate the first iterative value of  $T_{21}$  by Equation 26.
7. Calculate the  $T_{12}$  values with the  $T_{11}$  and  $T_{21}$  values.
8. Calculate the  $T_{22}$  value with the  $T_{12}$  and  $T_{21}$  values.
9. Compare the absolute temperature difference of all deviations that are less than  $0.05^\circ\text{C}$  as the final step of the calculation. Otherwise, repeat the computing from step 4.

### Evaluation of prediction performance

The criteria of the model evaluation were defined as follows:

1. Predictive errors

$$P_i = Y_i - X_i \quad (27)$$

where  $Y_i$  is the measurement temperature in  $^\circ\text{C}$  and  $X_i$  is the predicted temperature by thermal model in  $^\circ\text{C}$ .

2. Predictive performance

$$P_{\text{ave}} = \sum |P_i| / n \quad (28)$$

where  $|P_i|$  is the absolute value of  $P_i$  and  $n$  is the number of data.

## RESULTS AND DISCUSSION

### Predictive ability of model

A typical microclimate of the greenhouse for July 1, 2007 is presented in Figure 3a. Partly cloudy skies were found. The maximum solar radiation was nearly  $850 \text{ Wm}^{-2}$ . The maximum temperature was found at 14:30 pm. The external and internal shading nets were applied on this day. Roof vent and side vent were kept partially open and the air exchange rate by natural ventilation was nearly  $0.15 \text{ h}^{-1}$ .

As the solar radiation increased, the ambient temperature  $T_a$  is increased. The  $T_1$  values, air temperature of

upper layer was significant higher than that of  $T_2$  values, air temperature of lower layer. The maximum difference between  $T_1$  and  $T_a$  was  $10^\circ\text{C}$ . The maximum difference between  $T_2$  and  $T_a$  was  $6^\circ\text{C}$ . The transmittance of internal shading nets was 50%. As solar energy passed external shading nets and cover materials, 50% of the energy was entering the lower layer of the greenhouses. However, 50% of the energy was kept in the space that was enclosed by the cover materials and internal shading nets. The internal shading nets limited the air flow rate from the bottom of the greenhouse to the upper parts due to the natural ventilation effect. The heat accumulation was enhanced on increase of  $T_1$  value. Heat accumulation was also found in the lower layer. Some of the heat energy was transmitted to the upper layer due to the wind suction of natural ventilation. So the  $T_2$  value was lower than the  $T_1$  values.

The predictive values of  $T_1$  and  $T_2$  are shown in Figure 3b. The maximum difference between predicted values and  $T_1$  was  $2.8^\circ\text{C}$ . The  $P_{\text{ave}}$  value for  $T_1$  was  $1.3^\circ\text{C}$ . The maximum difference between predicted values and  $T_2$  was  $1.9^\circ\text{C}$ . The  $P_{\text{ave}}$  value for  $T_2$  was  $1.3^\circ\text{C}$ . Larger deviations between the predicted value and actual measured values were found in the early stage. The reason for this may be that the heat transfer of the ground was negligible. As the radiation energy entering was low, the amount of heat transfer into the greenhouse ground could be significant.

In the second observation, only the internal shading nets were utilized. The roof vent and side vent were kept in a fully open condition. The boundary of the air temperature and solar radiation is presented in Figure 4a. The temperature distribution and predicted values are indicated in Figure 4b. The  $T_1$  values were  $6^\circ\text{C}$  higher than the ambient temperatures. The  $T_2$  values were higher than  $T_a$  by  $2.7^\circ\text{C}$ . The maximum difference between two predictive temperatures was  $1.9^\circ\text{C}$  for  $T_1$ , and  $1.8^\circ\text{C}$  for  $T_2$ . The  $P_{\text{ave}}$  values for  $T_1$  and  $T_2$  were 1.1 and  $0.7^\circ\text{C}$ . Compared with Figure 3b, the predictive ability of the model was improved. This may be due to the fact that the increase of air exchange capacity by natural ventilation enhanced the predictive ability of the model.

In the third investigation, external and internal shading nets were applied. The boundary of the air temperature and solar radiation is presented in Figure 5a. Only the exhaust fans of the upper layer were operated. The temperature distribution and predictive values are shown in Figure 5b. The maximum temperature difference was  $4.2^\circ\text{C}$  for  $T_2$  and  $T_a$ , and  $2.1^\circ\text{C}$  for  $T_1$  and  $T_a$ . The  $P_{\text{ave}}$  values for two predictive temperatures were  $0.7^\circ\text{C}$  for  $T_1$  and  $0.5^\circ\text{C}$  for  $T_2$ . The operation of exhaust fans could draw in the ambient air into the upper layer to expel the heat accumulation. The release of heat accumulation could help the greenhouse air temperature to remain at a lower level.

In the fourth experiment, two shading nets and the exhaust fans installed at upper and lower layer were all

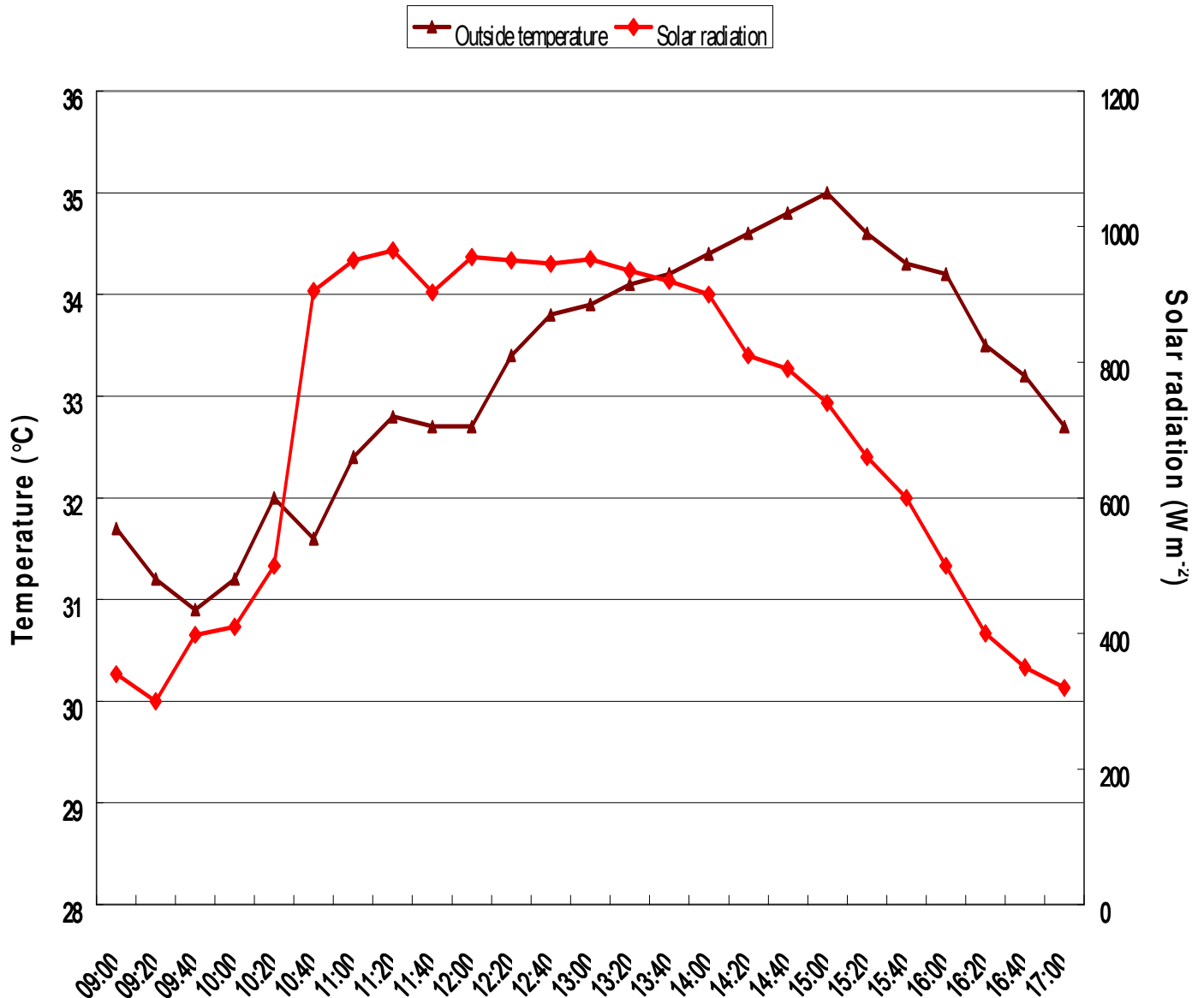


**Figure 3a.** The boundary of the air temperature and solar radiation for the first observation: ▲, outside temperature; ●, solar radiation; the roof and side vents were partially opened.

utilized. The boundary of the air temperature and solar radiation is presented in Figure 6a. The temperature distribution and predicted values from the model are shown in Figure 6b. The maximum difference between the  $T_1$  and  $T_a$  were 2.0°C. The difference between the temperature distribution curves of  $T_2$  and  $T_a$  were only 0.5°C. The operation of exhaust fans could draw in enough external air to surpass most of the heat accumulation in the lower layer. The  $T_2$  values were almost the same as the  $T_a$  values. The heat accumulation in the upper layer made the 2°C difference between  $T_2$  and  $T_a$ . The  $P_{ave}$  value was 0.6°C for  $T_1$  and 0.7°C for  $T_2$ . Comparing the results with other operating conditions,

the model had a good predictive performance at the higher ventilation rates.

### Sensitivity analysis of model

Typical weather conditions in the summer were used to simulate the temperature distribution in a greenhouse. The distribution of temperature and solar radiation is shown in Figure 7.

Three conditions were simulated; no ventilation, natural ventilation and mechanical ventilation. Under the first simulation conditions, no ventilation of greenhouse induced

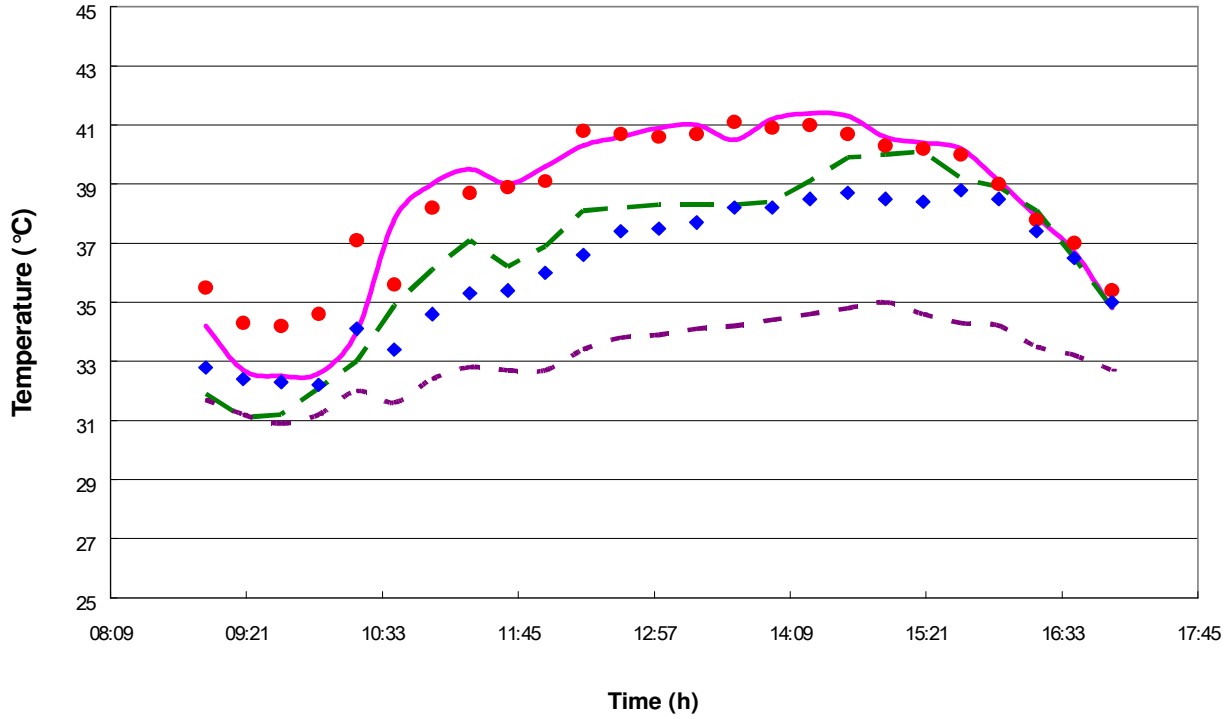


**Figure 3b.** The distribution of measured temperature and predictive temperature of model, the roof and side vents were partially opened: ●, measured temperature of upper layer; —, predicted temperature of upper layer; □, measured temperature of lower layer; - - - - , predicted temperature of lower layer; - - - - - , measured temperature of ambient air.

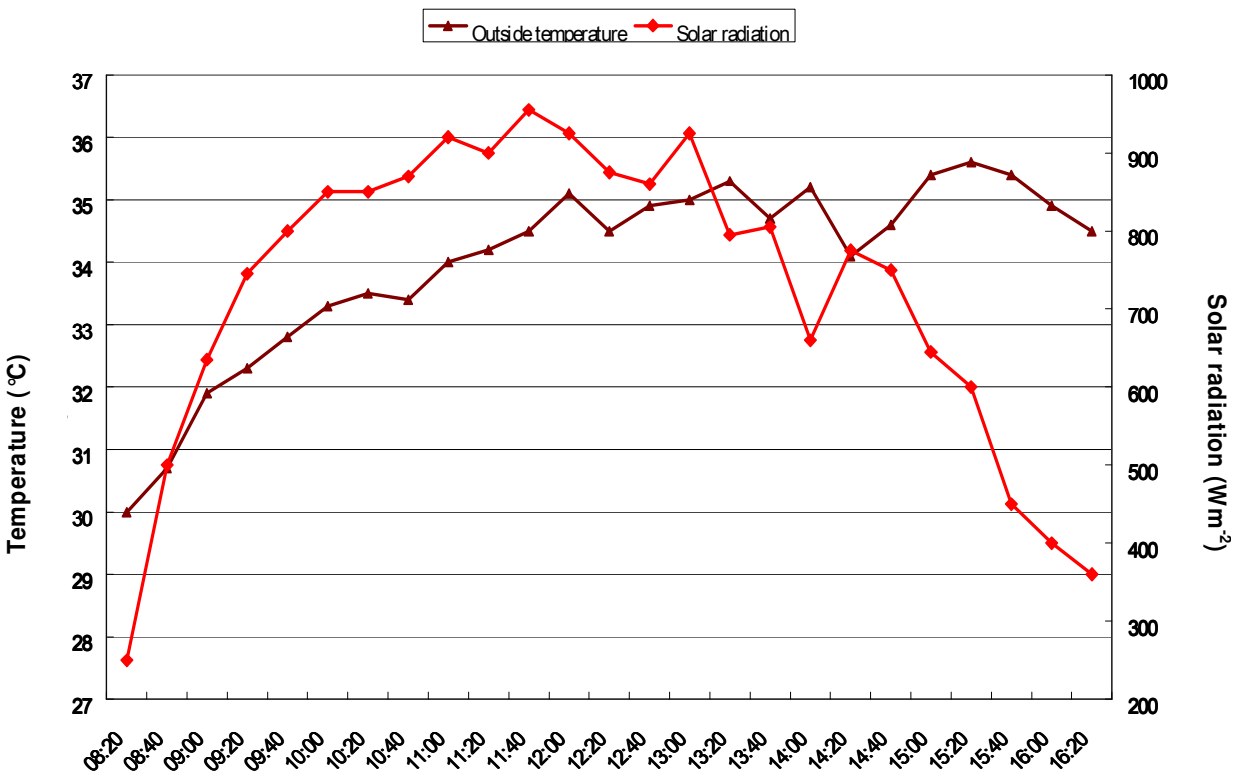


**Figure 4a.** The boundary of the air temperature and solar radiation for the second observation, ▲, outside temperature; ●, solar radiation; the roof and side vents were full opened.



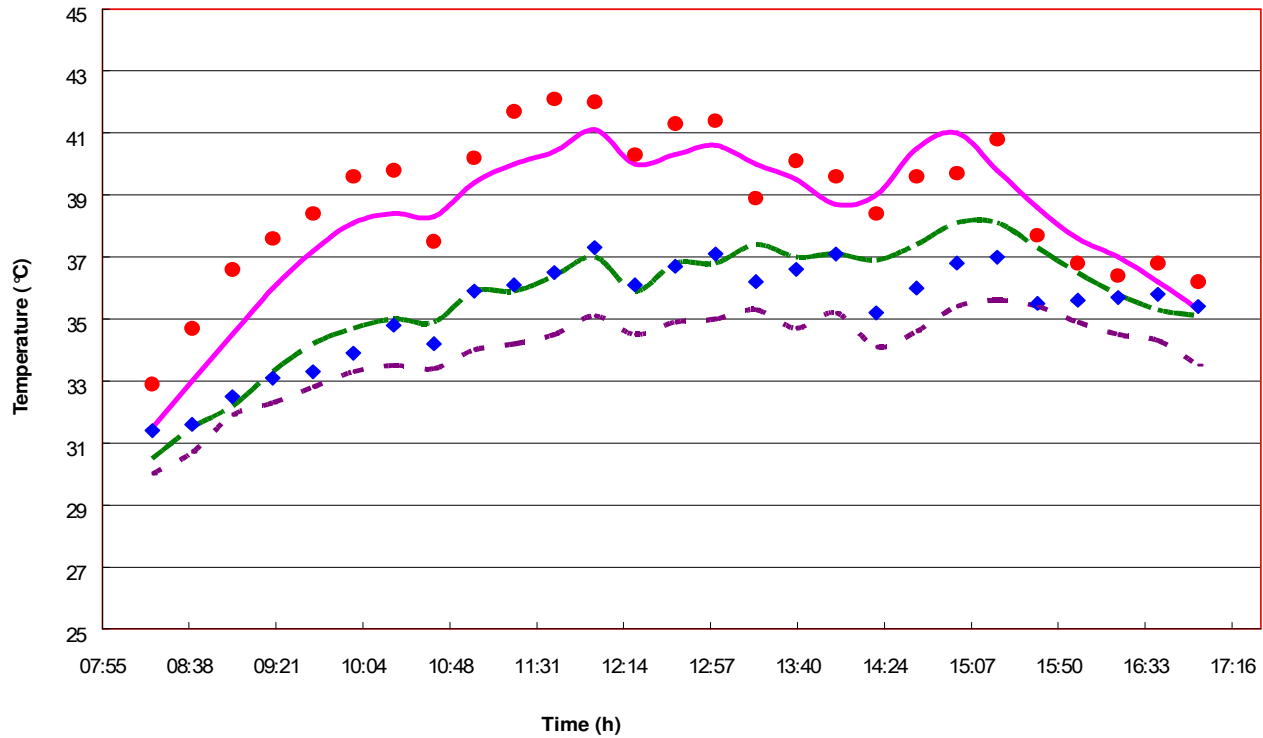


**Figure 4b.** The distribution of measured temperature and predictive temperature of model, the roof and side vents were fully opened: ●, measured temperature of upper layer; —, predicted temperature of upper layer; □, measured temperature of lower layer; — — —, predicted temperature of lower layer; - - - - -, measured temperature of ambient air.

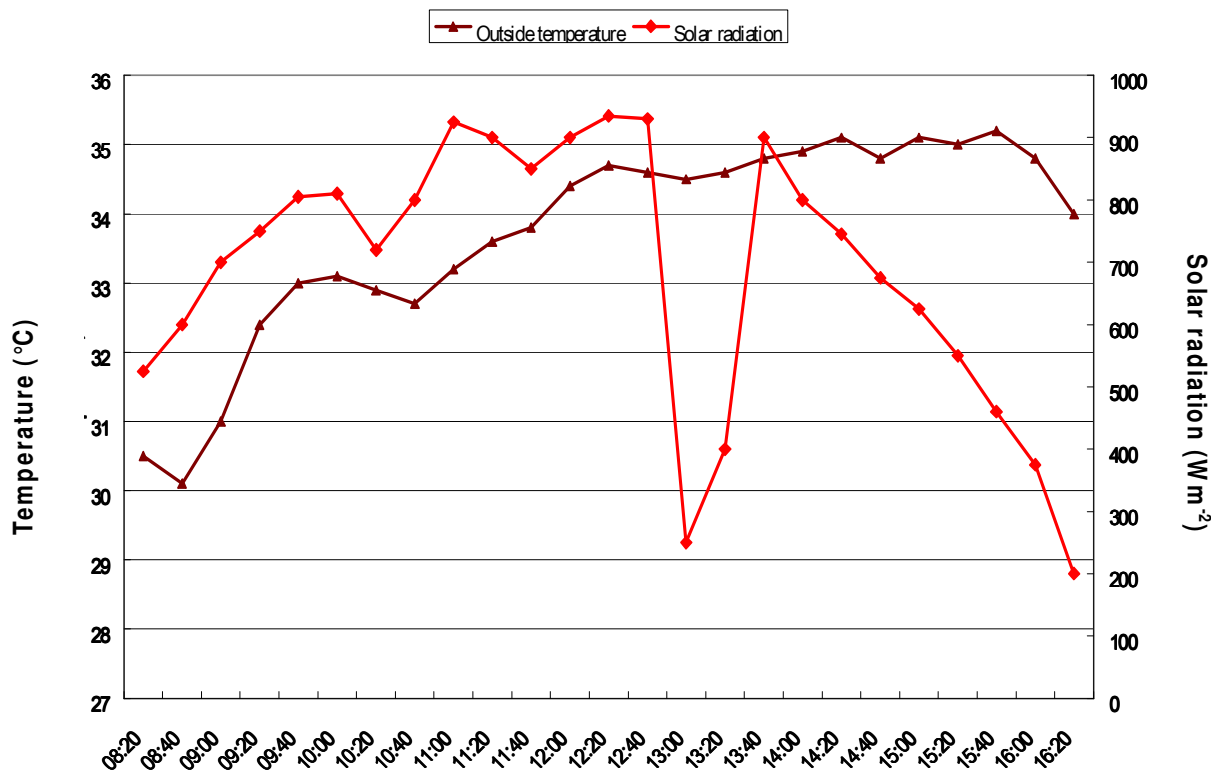


**Figure 5a.** The boundary of the air temperature and solar radiation for the third investigation, ▲, outside temperature; ●, solar radiation; the exhausted fans of upper layer were operated.

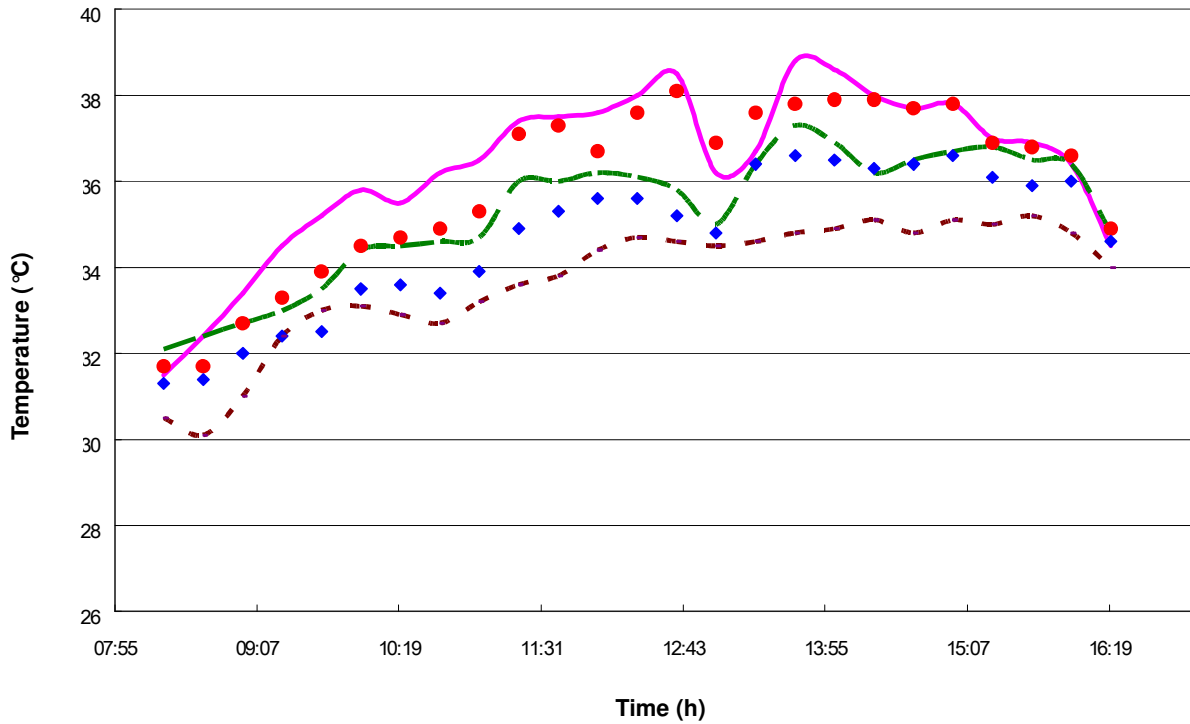


**Figure 5b.** The distribution of measured temperature and predictive temperature of model, the exhausted fans of upper layer were operated: ●, measured temperature of upper layer; —, predicted temperature of upper layer; □, measured temperature of lower layer; — — —, predicted temperature of lower layer; - - - - -, measured temperature of ambient air.

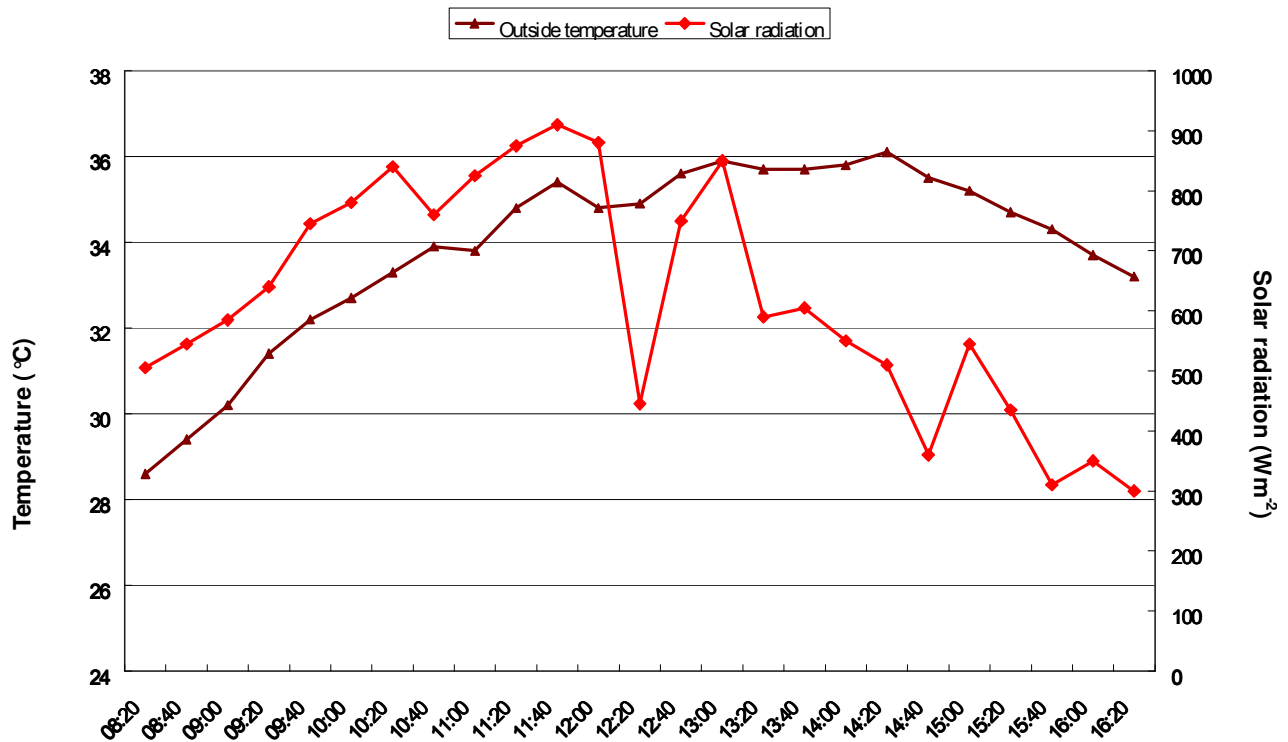


**Figure 6a.** The boundary of the air temperature and solar radiation for the fourth experiment, ▲, outside temperature; ●, solar radiation; the exhausted fans of upper and lower layer were operated.

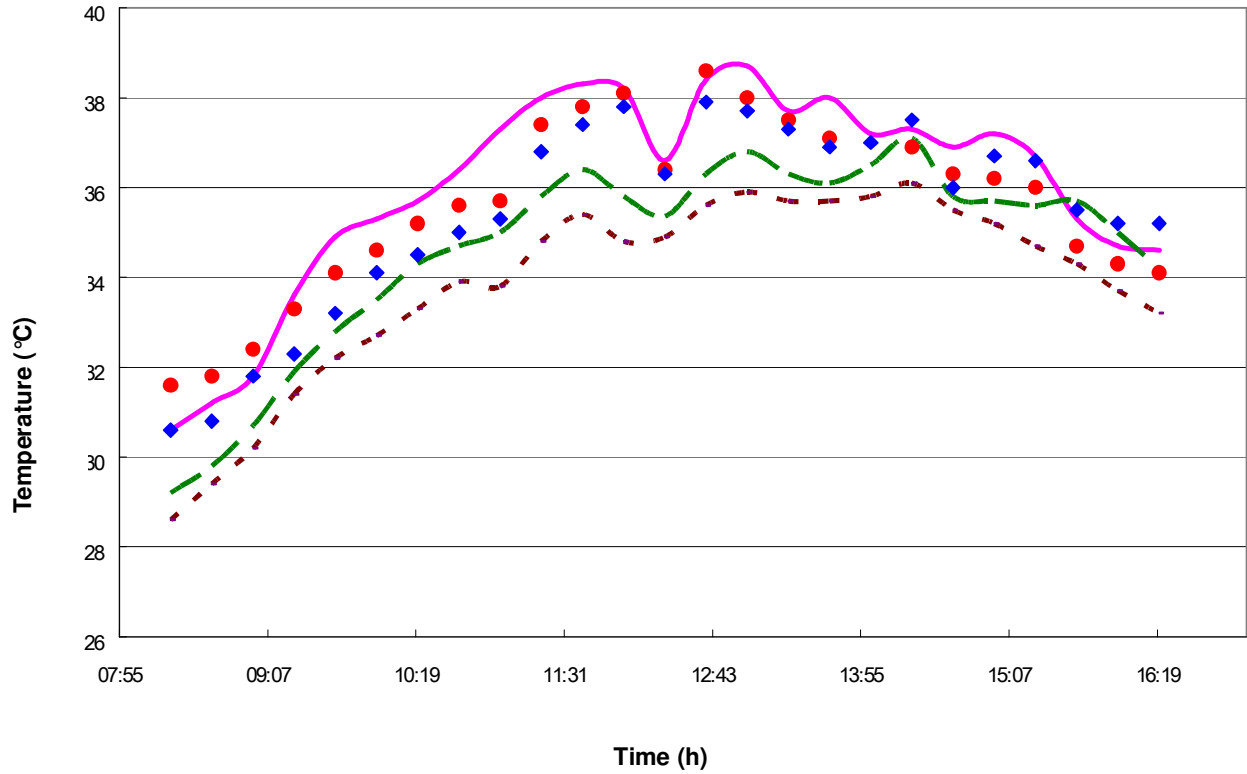


**Figure 6b.** The distribution of measured temperature and predictive temperature of model, the exhausted fans of upper and lower layer were operated: ●, measured temperature of upper layer; —, predicted temperature of upper layer; □, measured temperature of lower layer; - - -, predicted temperature of lower layer; - - - - -, measured temperature of ambient air.

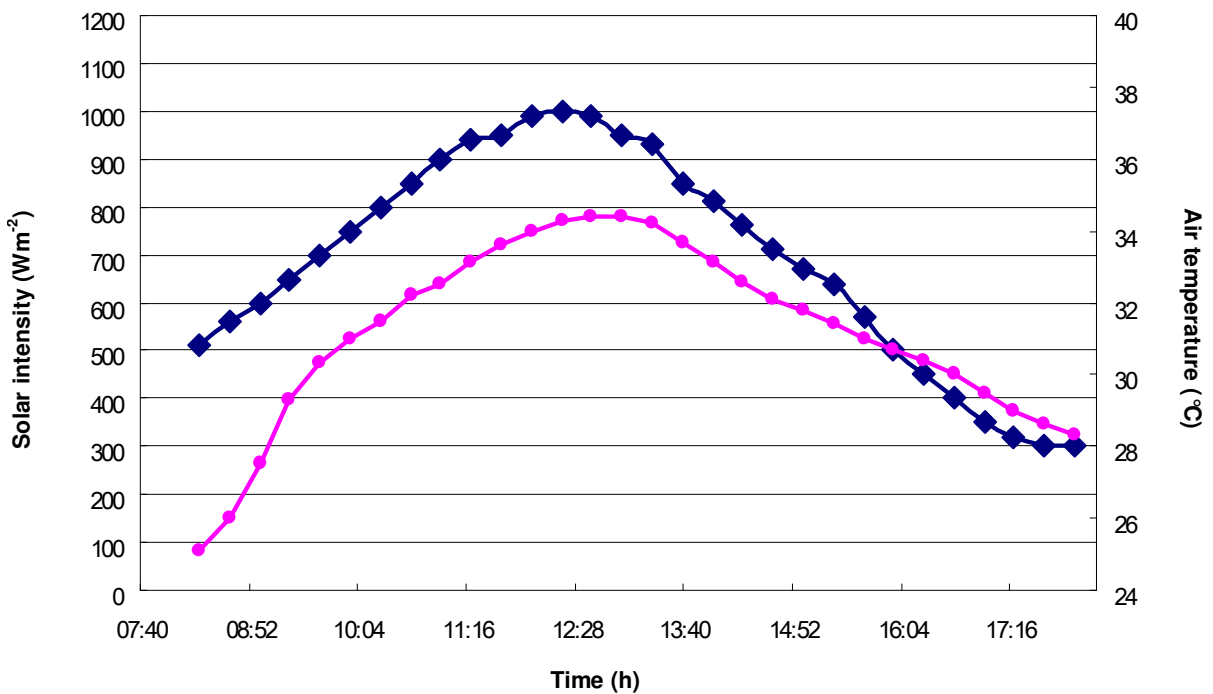


**Figure 7.** The distribution of temperature and solar intensity of ambient air for sensitive analysis: □, solar radiation; ■, ambient temperature.

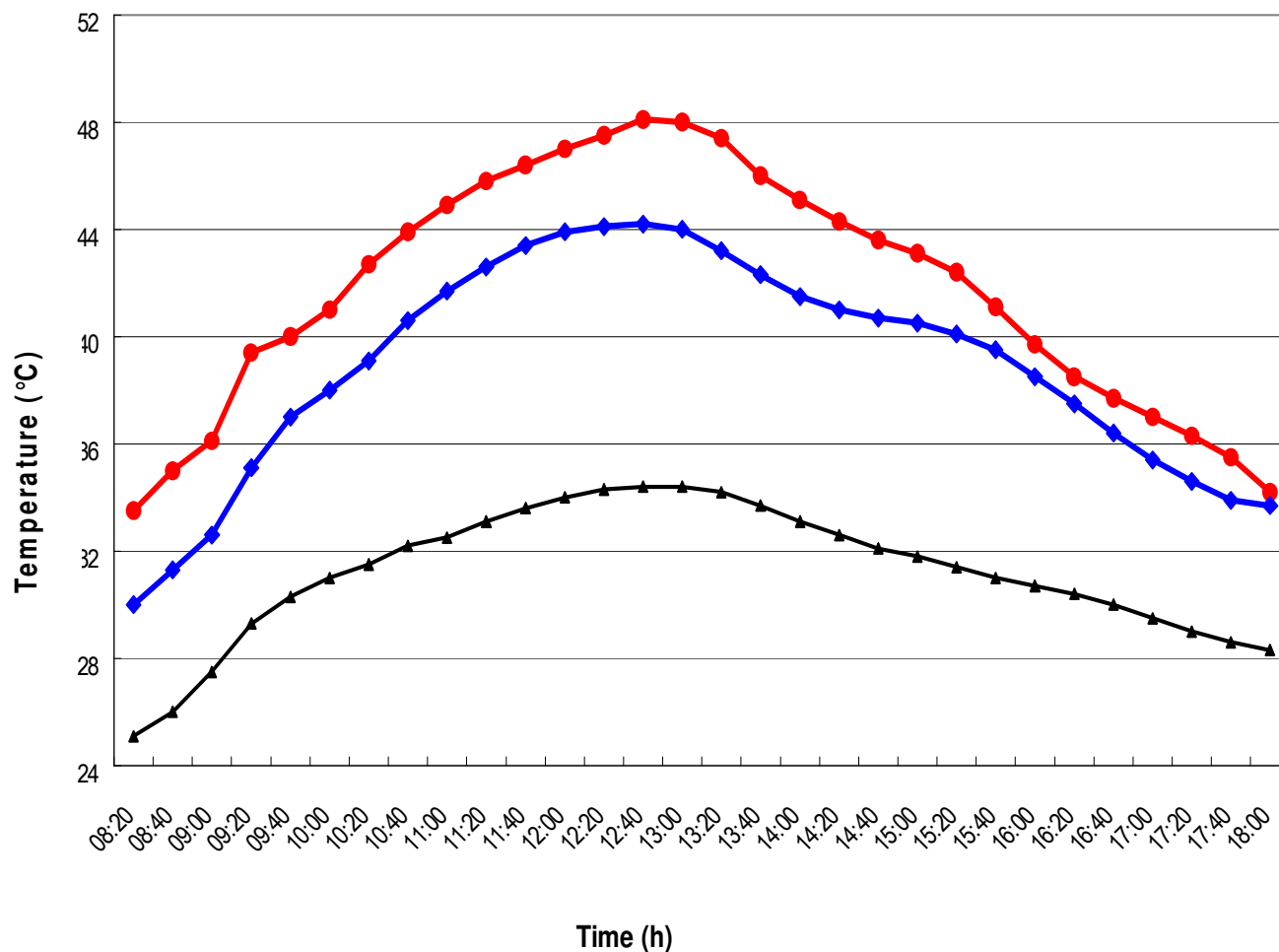


**Figure 8.** The distribution of the predictive temperature of model for sensitive analysis at the closed state of greenhouse: ●, upper temperature; □, lower temperature; ▲, ambient temperature.

a serious heat accumulation. The simulation result is presented in Figure 8. The shading nets only retarded the heat accumulation. However, only a small portion of the heat entering greenhouse could be transmitted to ambient environment by heat transfer. The temperature difference was larger than 20°C for  $T_1$  and  $T_a$ , and 16°C for  $T_2$  and  $T_a$ . As the air temperature was higher than 40°C, no commercial plant could survive under this serious heat stress.

In the second condition, the ambient air was induced into the greenhouse by natural ventilation. The effect of control technique is presented in Figure 9. The maximum difference between internal and external temperatures was 15°C for  $T_2$  and 10°C for  $T_1$ . The internal shading nets could decrease the amount of solar radiation entering. However, the nets retarded the air flow from the bottom to the roof. The function of natural ventilation could not release the heat accumulation effectively.

In the third condition, the amount of ambient air was sucked into the greenhouse by fans. The effect of control

technique is presented in Figure 10. The  $T_1$  values were 1.0°C higher than that of ambient air. The  $T_2$  values were almost the same as the ambient air temperature.

The purpose of application of greenhouse conditions in the summer was to grow the high value crops. From the simulation results of this model, a higher ventilation rate and reduction of solar radiation by shading nets was significant in reducing the air temperature in a greenhouse. Utilization of shading nets only, did not help the heat release in the greenhouse. The cooling performance with the shading nets and mechanical ventilation reduced the interior temperature of the greenhouse to a level similar to ambient atmosphere temperature.

## Conclusions

A simple greenhouse climate model was developed in this study that considered the effect of shading nets. The model was used to consider the effect of ventilation rate

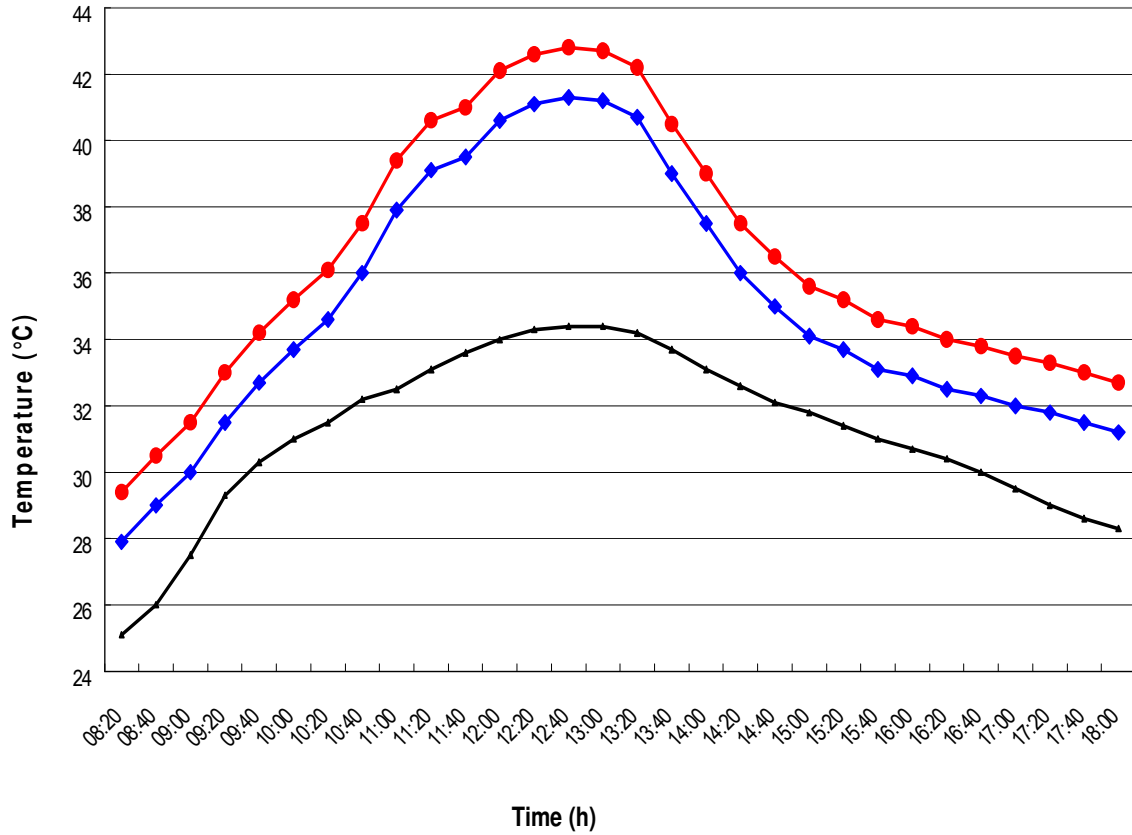


**Figure 9.** The distribution of the predictive temperature of model for sensitive analysis by natural ventilation: ●, upper temperature; □, lower temperature; ▲, ambient temperature.

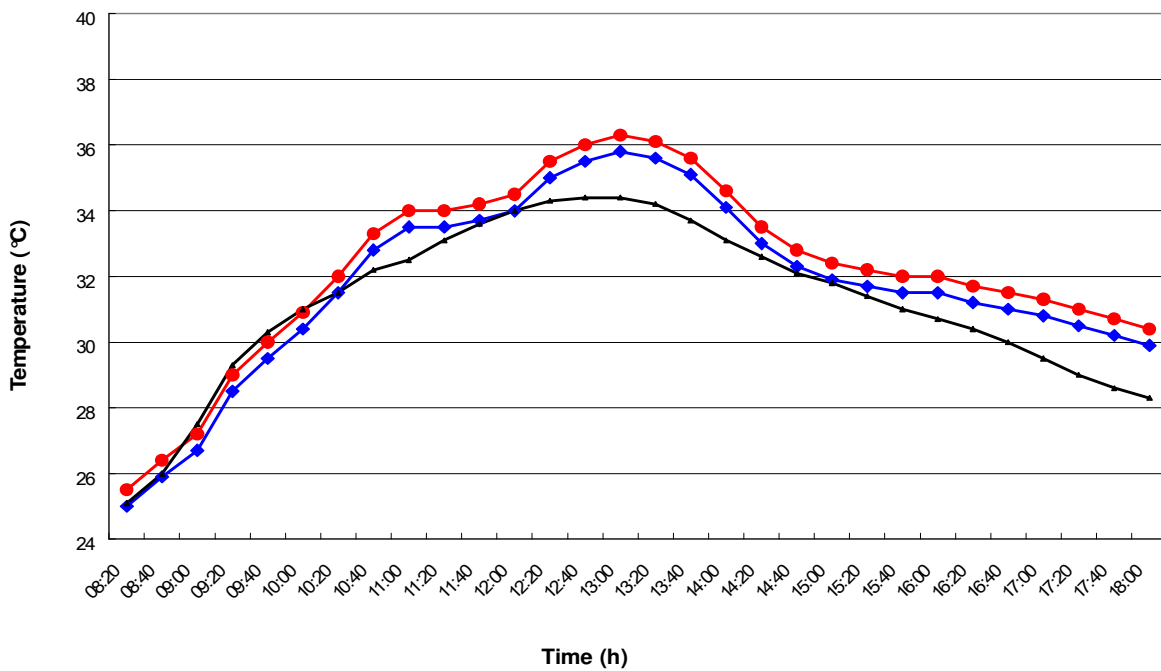


**Figure 10.** The distribution of the predictive temperature of model for sensitive analysis by forced ventilation: ●, upper temperature; □, lower temperature; ▲, ambient temperature.

and shading function. This model was validated by data measured in a greenhouse with tomatoes. A close agreement was found between the predictive values and measured values. The application of the model by sensitivity analysis revealed that the combination of shading application and higher ventilation rates was the best way to reduce the internal temperature of a greenhouse during the summer months.

## Notation

**a**, constant; **A<sub>1</sub>**, surface area of the upper layer included the roof and partial wall, m<sup>2</sup>; **A<sub>2</sub>**, wall area of the lower part, m<sup>2</sup>; **A<sub>f</sub>**, floor area, m<sup>2</sup>; **A<sub>op</sub>**, area of opening, m<sup>2</sup>; **A<sub>s</sub>**, area of internal shading nets, m<sup>2</sup>; **AR**, natural air exchange rate of the greenhouse, m<sup>3</sup>s<sup>-1</sup>; **C<sub>d</sub>**, discharge coefficient value; **C<sub>p</sub>**, air specific heat, J kg<sup>-1</sup>°C<sup>-1</sup>; **F<sub>1s</sub>**, shape factors for the sky as seen from the upper layer; **F<sub>2s</sub>**, shape factors for the sky as seen from the lower layer; **g**, gravitational acceleration, ms<sup>-2</sup>; **H**, opening height, m; **h<sub>t</sub>**, constant; **I<sub>s</sub>**, Incoming shortwave radiation, Wm<sup>-2</sup>; **LAI**, leaf area index; **M<sub>1</sub>**, ventilation rate of mechanical devices in the upper part, m<sup>3</sup>s<sup>-1</sup>; **M<sub>2</sub>**, ventilation rate of mechanical devices in the lower part, m<sup>3</sup>s<sup>-1</sup>; **M<sub>12</sub>**, ventilation rate between the upper and lower layer due to the mechanical ventilation of the upper layer, m<sup>3</sup>s<sup>-1</sup>; **M<sub>21</sub>**, ventilation rate between the upper and lower part due to the mechanical ventilation of the lower layer, m<sup>3</sup>s<sup>-1</sup>; **n**, number of data; **P<sub>ave</sub>**, predictive performance, °C; **P<sub>f</sub>**, Canopy area index; **P<sub>i</sub>**, predictive error, °C; **P<sub>ws</sub>**, air saturated vapor pressure, kPa; **RH**, relative humidity, %; **T<sub>1</sub>**, upper layer temperature, °C; **T<sub>1k</sub>**, absolute air temperature of the upper layer air, K; **T<sub>2</sub>**, lower layer temperature, °C; **T<sub>2k</sub>**, absolute air temperature of lower part, K; **T<sub>a</sub>**, ambient temperature, °C; **T<sub>ak</sub>**, ambient air temperature, K; **T<sub>ave</sub>**, average temperature of greenhouse, °C; **Tr**, transpiration rate of tomatoes, kgm<sup>-2</sup>s<sup>-1</sup>; **T<sub>sky</sub>**, sky temperature, K; **U<sub>12</sub>**, heat transfer coefficient of internal shading nets, Wm<sup>-2</sup>°K<sup>-1</sup>; **U<sub>k2</sub>**, heat transfer coefficient of cover materials, Wm<sup>-2</sup>°K<sup>-1</sup>; **U<sub>w1</sub>**, heat transfer coefficient of greenhouse cover materials, Wm<sup>-2</sup>°K<sup>-1</sup>; **V<sub>1</sub>**, volume of the upper layer, m<sup>3</sup>; **V<sub>2</sub>**, volume of the lower layer, m<sup>3</sup>; **X<sub>i</sub>**, predicted temperature by thermal model, °C; **Y<sub>i</sub>**, measurement temperature, °C; **|Pi|**, absolute values of predictive error; **α**, absorptance of internal nets; **ρ**, air density, kgm<sup>-3</sup>; **σ**, Stephan-Boltzman constant; **ε**, long wave thermal transmittance of cover materials; **τ<sub>0</sub>**, transmittance of external shading nets; **τ<sub>1</sub>**, transmittance of internal shading nets; **λ**, latent heat of vaporization, kJkg<sup>-1</sup>; **γ**, thermodynamic psychrometric constant, kPa K<sup>-1</sup>.

## REFERENCES

- Boulard T, Baille A (1993). A simple greenhouse climate control model incorporating effects of ventilation and evaporative cooling. *Agr. For. Meteorol.* 65: 145-157.
- Boulard TH, Lagier FJ, Fargues J, Smits S, Rougier M, Jeannequin B (2004). Effects of greenhouse ventilation on humidity of indoor air and in leaf boundary-layer. *Agric. For. Meteorol.* 125: 225-239.
- Chen C (2003). Thermal and moisture gradient model for greenhouse. *Agric. Eng. J.* 12: 143-164.
- Critten DL, Bailey BJ (2002). A review of greenhouse engineering developments during the 1990s. *Agric. For. Meteorol.* 112: 1-22.
- Demrati H, Boulard T, Fatnassi H, Bekkaoui A, Majdoubi H, Elattir H, Bouriden L (2007). Microclimate and transpiration of a greenhouse banana crop. *Biosyst. Eng.* 98: 66-78.
- Emekli NY, Kendirli B, Kurunc A (2010). Structural analysis and functional characteristics of greenhouses in the Mediterranean region of Turkey. *Afr. J. Biotechnol.* 9:3131-3139.
- Fatnassi H, Noulard T, Bouriden L (2003). Simulation of climate conditions in full-scale greenhouse fitted with insect-proof screens. *Agric. For. Meteorol.* 118: 97-111.
- Froehlich DP, Albright LD, Scott NR, Chandra P (1979). Steady-periodic analysis of glasshouse thermal environment. *Trans. ASAE*, 22: 387-399.
- Impron I, Hemming S, Bot GPA (2007). Simple greenhouse climate model as a design tool for greenhouses in tropical lowland. *Biosyst. Eng.* 69: 79-89.
- Jolliet O (1994). Hortitrans, a model for predicting and optimizing humidity and transpiration in greenhouses. *J. Agric. Eng. Res.* 57: 23-37.
- Kano A, Sadler E (1985). Survey of greenhouse models. *J. Agric. Meteorol.* 41: 75-81.
- Omer AM (2009). Constructions, applications and the environment of greenhouses. *Afr. J. Biotechnol.* 8: 7205-7227.
- Oz H, Atilgan A, Buyuktas K, Alagoz T (2009). The efficiency of fan-pad cooling system in greenhouse and building up of internal greenhouse temperature map. *Afr. J. Biotechnol.* 8: 5436-5444.
- Roy JC, Boulard Y, Kittas C, Wang S (2002). Convective and ventilation transfers in greenhouses, Part 1: the greenhouse considered as a perfectly stirred tank. *Biosyst. Eng.* 83: 1-20.
- USAID (2008). Protected Agriculture in Jamaica: A Reference Manual. 1st ed. New York, USA: Unites States Agency for International Development.
- Sengar SH, Kothari S (2008). Thermal modeling and performance evaluation of arch shape greenhouse for nursery raising. *Afr. J. Math. Comp. Sci. Res.* 1: 1-9.
- Sethi VP, Sharma SK (2007). Survey of cooling technologies for worldwide agricultural greenhouse applications. *Solar Energy*, 81: 1447-1459.
- Weiss A (1977). Algorithms for the calculation of moist air properties on a hand calculator. *Trans. ASAE*, 20: 1133-1136.
- Van Heum E, Van Der Post K (2004). Protected cultivation. 1st ed. the Netherlands, Digigraft Publ., Wageningen.